

TESS Data Release Notes: Sector 98, DR134

*Benjamin M. Tofflemire, Marziye Jafariyazani, Douglas A. Caldwell, Joseph D. Twicken
SETI Institute, Mountain View, California*

*Jon M. Jenkins
NASA Ames Research Center, Moffett Field, California*

*Roland Vanderspek
Kavli Institute for Astrophysics and Space Science, Massachusetts Institute of Technology,
Cambridge, Massachusetts*

*Michael M. Fausnaugh
Texas Tech University, Lubbock, Texas*

*Stephanie Striegel
SETI Institute, Mountain View, California*

*Nicole Schanche
University of Maryland at College Park, College Park, Maryland
NASA Goddard Space Flight Center, Greenbelt, Maryland*

NASA STI Program ... in Profile

Since its founding, NASA has been dedicated to the advancement of aeronautics and space science. The NASA scientific and technical information (STI) program plays a key part in helping NASA maintain this important role.

The NASA STI program operates under the auspices of the Agency Chief Information Officer. It collects, organizes, provides for archiving, and disseminates NASA's STI. The NASA STI program provides access to the NTRS Registered and its public interface, the NASA Technical Reports Server, thus providing one of the largest collections of aeronautical and space science STI in the world. Results are published in both non-NASA channels and by NASA in the NASA STI Report Series, which includes the following report types:

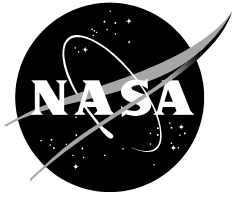
- **TECHNICAL PUBLICATION.** Reports of completed research or a major significant phase of research that present the results of NASA Programs and include extensive data or theoretical analysis. Includes compilations of significant scientific and technical data and information deemed to be of continuing reference value. NASA counterpart of peer-reviewed formal professional papers but has less stringent limitations on manuscript length and extent of graphic presentations.
- **TECHNICAL MEMORANDUM.** Scientific and technical findings that are preliminary or of specialized interest, e.g., quick release reports, working papers, and bibliographies that contain minimal annotation. Does not contain extensive analysis.
- **CONTRACTOR REPORT.** Scientific and technical findings by NASA-sponsored contractors and grantees.

- **CONFERENCE PUBLICATION.** Collected papers from scientific and technical conferences, symposia, seminars, or other meetings sponsored or co-sponsored by NASA.
- **SPECIAL PUBLICATION.** Scientific, technical, or historical information from NASA programs, projects, and missions, often concerned with subjects having substantial public interest.
- **TECHNICAL TRANSLATION.** English-language translations of foreign scientific and technical material pertinent to NASA's mission.

Specialized services also include organizing and publishing research results, distributing specialized research announcements and feeds, providing information desk and personal search support, and enabling data exchange services.

For more information about the NASA STI program, see the following:

- Access the NASA STI program home page at <http://www.sti.nasa.gov>
- E-mail your question to help@sti.nasa.gov
- Phone the NASA STI Information Desk at 757-864-9658
- Write to:
NASA STI Information Desk
Mail Stop 148
NASA Langley Research Center
Hampton, VA 23681-2199



TESS Data Release Notes: Sector 98, DR134

*Benjamin M. Tofflemire, Marziye Jafariyazani, Douglas A. Caldwell, Joseph D. Twicken
SETI Institute, Mountain View, California*

*Jon M. Jenkins
NASA Ames Research Center, Moffett Field, California*

*Roland Vanderspek
Kavli Institute for Astrophysics and Space Science, Massachusetts Institute of Technology,
Cambridge, Massachusetts*

*Michael M. Fausnaugh
Texas Tech University, Lubbock, Texas*

*Stephanie Striegel
SETI Institute, Mountain View, California*

*Nicole Schanche
University of Maryland at College Park, College Park, Maryland
NASA Goddard Space Flight Center, Greenbelt, Maryland*

Acknowledgements

These Data Release Notes provide information on the processing and export of data from the Transiting Exoplanet Survey Satellite (TESS). The data products included in this data release are full frame images (FFIs), target pixel files, light curve files, collateral pixel files, cotrending basis vectors (CBVs), and Data Validation (DV) reports, time series, and associated xml files.

These data products were generated by the TESS Science Processing Operations Center (SPOC, [Jenkins et al., 2016](#)) at NASA Ames Research Center from data collected by the TESS instrument, which is managed by the TESS Payload Operations Center (POC) at Massachusetts Institute of Technology (MIT). The format and content of these data products are documented in the [Science Data Products Description Document \(SDPDD\)](#). The SPOC science algorithms are based heavily on those of the Kepler Mission science pipeline, and are described in the [Kepler Data Processing Handbook \(Jenkins, 2020\)](#). The Data Validation algorithms are documented in [Twicken et al. \(2018\)](#) and [Li et al. \(2019\)](#). The [TESS Instrument Handbook \(Vanderspek et al., 2018\)](#) contains more information about the TESS instrument design, detector layout, data properties, and mission operations.

The TESS Mission is funded by NASA's Science Mission Directorate.

1 Observations

TESS Sector 98 represents the second four-orbit sector observation of a single field of view, including physical orbits 205, 206, 207 and 208 of the spacecraft around Earth. The longer sector is intended to permit discovery of longer-period planets and investigations of other longer timescale astrophysical phenomena than the nominal ~ 27 -day sectors support.

In this sector, data collection was paused for 1.46 days to download data. Data were downloaded approximately every seven days, near apogee and perigee of each orbit. In total, there are 55.94 days of science data collected in Sector 98.

Table 1: Sector 98 Observation times

	UTC	TJD ^a	Cadence #
Orbit 205a start	2025-11-08 23:49:20	3988.49339	1987948
Orbit 205a end	2025-11-16 02:29:20	3995.60450	1993067
Orbit 205b start	2025-11-16 07:29:20	3995.81284	1993218
Orbit 205b end	2025-11-23 07:03:20	4002.79478	1998244
Orbit 206a start	2025-11-23 12:05:20	4003.00450	1998396
Orbit 206a end	2025-11-30 07:39:19	4009.81977	2003302
Orbit 206b start	2025-11-30 12:39:19	4010.02811	2003453
Orbit 206b end	2025-12-07 09:09:19	4016.88227	2008387
Orbit 207a start	2025-12-07 14:09:19	4017.09060	2008538
Orbit 207a end	2025-12-14 19:23:19	4024.30866	2013734
Orbit 207b start	2025-12-15 00:25:19	4024.51838	2013886
Orbit 207b end	2025-12-22 02:03:18	4031.58643	2018974
Orbit 208a start	2025-12-22 07:05:18	4031.79615	2019126
Orbit 208a end	2025-12-29 03:03:18	4038.62809	2024044
Orbit 208b start	2025-12-29 08:05:18	4038.83782	2024196
Orbit 208b end	2026-01-05 09:33:18	4045.89892	2029279

^a TJD = TESS JD = JD - 2,457,000.0

(The horizontal black lines mark gaps in the light curves for data downlink.)

The spacecraft pointing was set to RA (J2000): 80.166°; Dec (J2000): -31.055°; Roll: 186.639°. See the TESS project [Sector 98 observation page](#)¹ for the coordinates of the spacecraft pointing and center field-of-view of each camera. Fields-of-view for each camera can be found at the TESS Guest Investigator Office [observations status page](#).² Additional details for Guest Investigator target lists selected for 2-minute and 20-second observations can be found at the [Sector 98 observation page](#) and the [observations status page](#).

¹<https://tess.mit.edu/observations/sector-98>

²<https://heasarc.gsfc.nasa.gov/docs/tess/sector.html>

1.1 Targets and Light Curves

There were 2438 targets chosen for 20-second cadence observations and 13000 targets chosen for 2-minute cadence observations. Table 2 provides targets that were not fully processed with the photometric pipeline as well as targets that were fully processed but received warnings during aperture assignment.

For targets that were not processed with the photometric pipeline, the target pixel files with original and calibrated pixel data are provided, but no light curves are produced. Note that the target pixel files do not include a background correction for stars without light curves. The most common reason for a target to not be processed with the photometric pipeline is that the target exceeds a brightness threshold ($T_{\text{mag}} \lesssim 1.8$) that results in large pixel stamps. A target located too close to a very bright star, having a comparably bright companion, impacted by saturated star bleed trails, or having an error in identifying a clean background region are less common causes for a target to not be processed with the photometric pipeline. Visual examination of the target along with custom aperture selection may be needed for photometric analysis of the impacted targets. Warnings during aperture assignment occur when the aperture is discontinuous or clipped, and the resulting photometry is expected to be unreliable.

The distribution of 2-minute targets in sector Sector 98 was skewed more heavily toward faint targets compared to a typical sector. The median magnitude of 2-min targets in a typical sector is $T_{\text{mag}} \sim 10.7$ mag (assessed from Sectors 94, 95, 96). The median magnitude in the present sector is $T_{\text{mag}} \sim 13.5$ mag, driven by a large number of targets with T_{mag} between 17 and 20. Large quantities of faint targets can negatively impact the performance of systematic error correction (PDC) and they are less amenable to transit searches for small planets. Figure 5 has been expanded to capture the photometric performance of the faint population. We note that this shift toward fainter targets was also present in Sector 97.

Table 2: TIC IDs for targets without light curves and photometric aperture warnings

No Light Curve Generated		Aperture Warning	
2-minute	20-second	2-minute	20-second
38877693	46312112		93279196
46312112	231308237		300015238
231308237	255559489		300015239
238196512			
255559489			
672009090			
708357666			
708565082			

1.2 Spacecraft Pointing and Momentum Dumps

The pointing in Sector 98 was set at -54.0 degrees in ecliptic latitude. Camera 4 was pointed near the South Ecliptic Pole. Camera 1 was used for guiding in second half of each orbit:

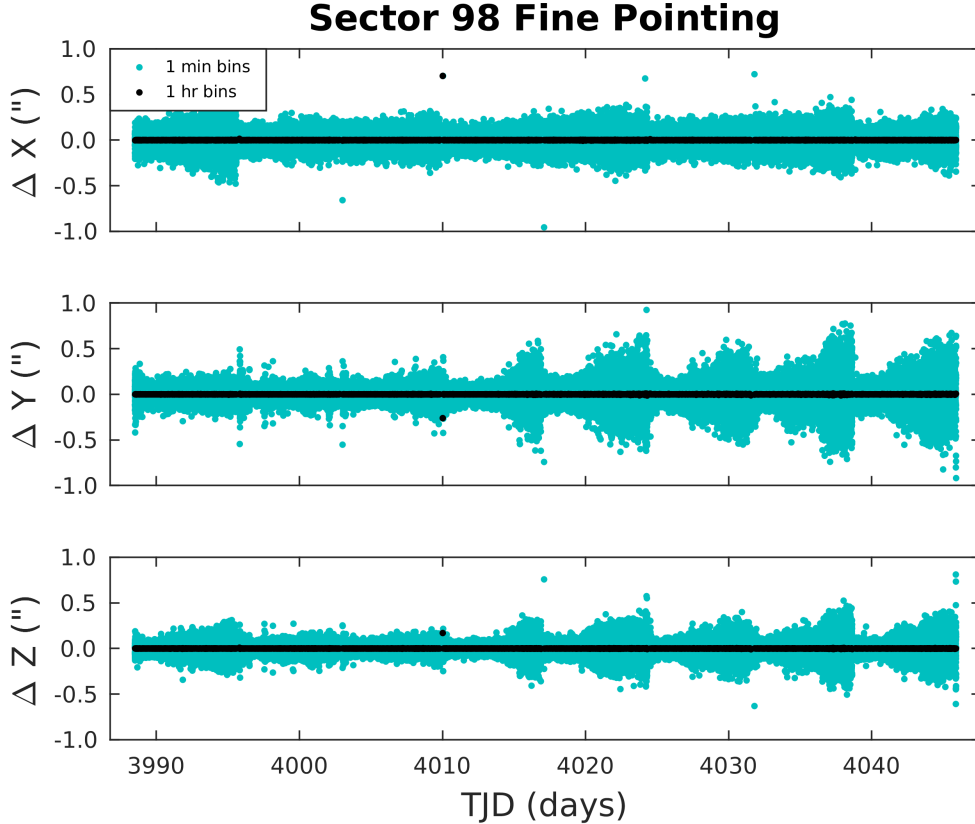


Figure 1: The delta-quaternions from each camera have been converted to spacecraft frame, binned to 1 minute and 1 hour, averaged across cameras. Long-term trends (such as those caused by differential velocity aberration) have also been removed. The $\Delta X/\Delta Y$ directions represent offsets along the detectors’ rows/columns, while the ΔZ direction represents spacecraft roll.

205b, 206b, 207b, and 208b. Camera 4 was also used for guiding in all eight half-orbit segments. Two momentum dumps were performed in each orbit. The momentum dumps are performed at the end of each data downlink just before data collection resumes. Data impacted by momentum dumps and data downlinks are marked with data quality flags (see Appendix A). Figure 1 summarizes the pointing performance over the course of the sector based on Fine Pointing telemetry.

1.3 Scattered Light

Figure 2 shows the median value of the background estimate for all targets on a given CCD as a function of time. Times of high background correspond to times when the Earth and/or Moon approach the camera’s field of view causing scattered light from these bright objects to enter the cameras. The viewing geometry of the Earth and Moon relative to TESS’s pointing in Sector 98 are shown in Figure 3. Figure 3 shows the angle between each camera’s boresight and the Earth or Moon—this figure can be used to identify periods affected by scattered light and the relative contributions of the Earth and Moon to the image backgrounds. Scattered light increases as the camera boresight angle between the Earth and Moon is $\lesssim 35^\circ$ and will

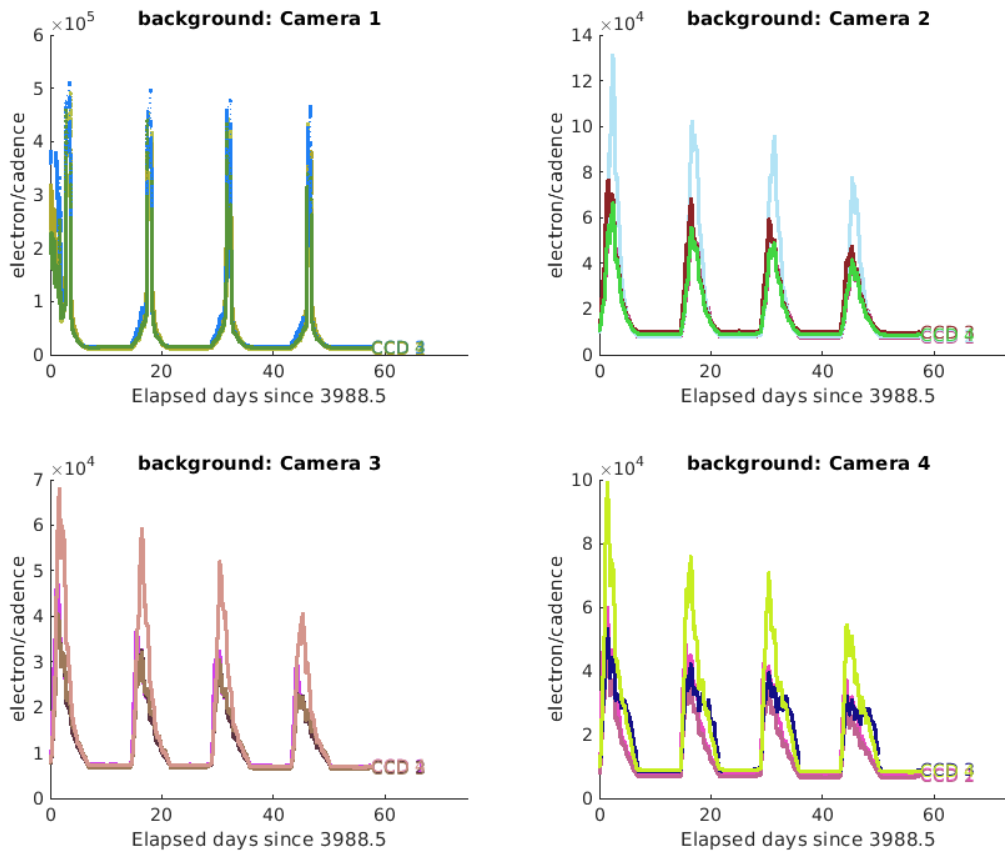


Figure 2: Median background flux across all targets on a given CCD in each camera. The changes are caused by variations in the orientation and distance of the Earth and Moon.

strongly impact photometric observations for angles $\lesssim 25^\circ$. Data impacted by scattered light are marked with data quality flags (see Appendix A).

1.4 Smear Correction Contamination

Due to the shutterless operation of the TESS instrument (see [TESS Instrument Handbook](#), §9.5), data calibration involves subtracting a smear correction. The “smear rows” are virtual pixels (not physical pixels) that provide an estimate of the contaminating flux that accumulates in each pixel during the ~ 0.02 s shutterless frame transfer. The smear correction, estimated from the smear rows, is subtracted from the whole column. However, bright stars located in the science frame, upper buffer rows, and lower science frame rows can bleed into the smear rows resulting in an overestimated smear correction. An overestimated smear correction in calibrated data products can be identified by one or more consecutive columns that are anomalously dark relative to neighboring columns, whereas the raw/uncalibrated images do not reveal an anomalously dark column relative to its neighbors. Mitigating an overestimated smear correction may require a custom calibration that robustly interpolates

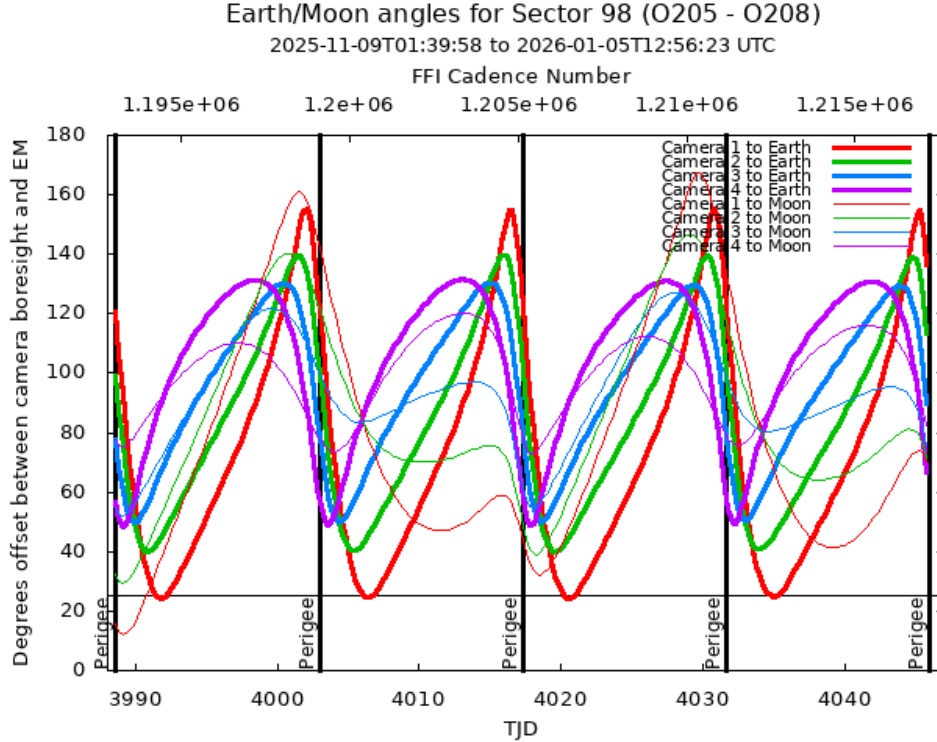


Figure 3: Angle between the four camera boresights and the Earth/Moon as a function of time. When the Earth is within $\sim 25^\circ$ of a camera’s boresight, transiting planet searches may be compromised by high levels of scattered light. At larger angles, up to $\sim 35^\circ$, scattered light patterns and complicated structures may be visible. At yet larger angles, low level patchy features may be visible. Scattered light from the Moon is generally only noticeable below $\sim 35^\circ$. This figure can be used to identify periods affected by scattered light and the relative contributions of the Earth and Moon to the background. However, the background intensity and locations of scattered light features depend on additional factors, such as the Earth/Moon azimuth and distance from the spacecraft.

across the contaminated smear columns or a robust smear estimate from the science frame.

1.5 Data Anomaly Flags

The [SDPDD](#) (§9) lists data quality flags and the associated binary values used for TESS data. Appendix A describes each Data Anomaly Flag in more detail.

2 Pipeline Performance and Results

2.1 Light Curves and Photometric Precision

Figure 4 shows an assessment of the PDC systematic error correction of the pipeline by comparing simple aperture photometry light curves from PA and the PDC systematic-error corrected light curves. Figure 5 shows the achieved Combined Differential Photometric Pre-

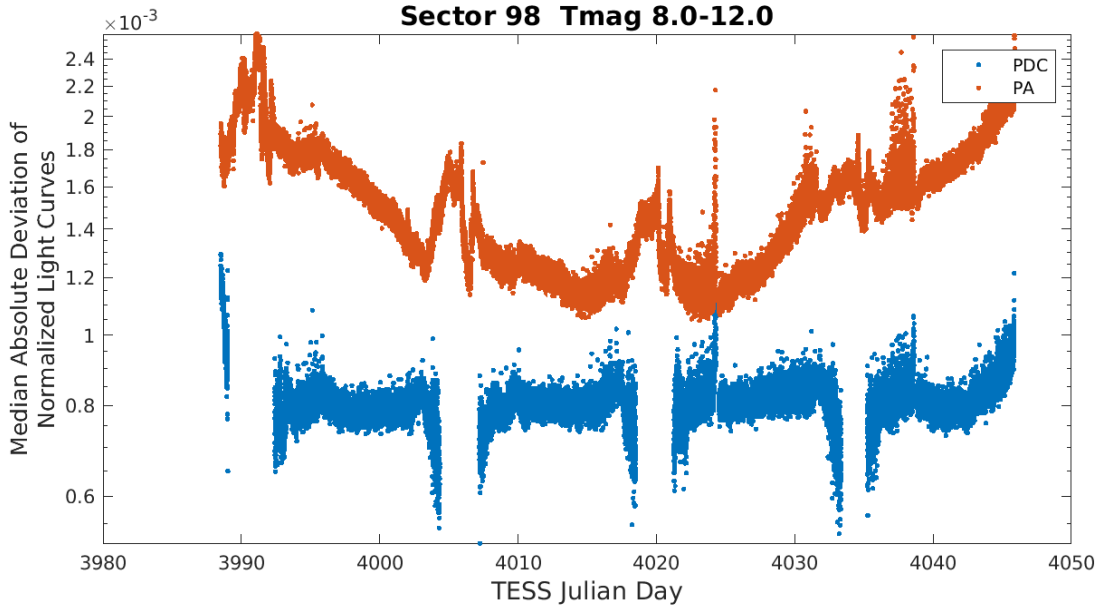


Figure 4: Median absolute deviation (MAD) for the two-minute cadence data from Sector 98, showing the performance of the cotrending after identifying Manual Exclude data quality flags. The MAD is calculated in each cadence across stars with flux variations less than 1% for both the PA (red) and PDC (blue) light curves, where each light curve is normalized by its median flux value. The scatter in the PA light curves is much higher than that for the PDC light curves, and the outliers in the PA light curves are largely absent from the PDC light curves due to the use of the anomaly flags.

cision (CDPP) at 1-hour timescales for two-minute targets. We encourage users to examine several light curve quality assessment values (CROWDSAP, PDC_TOT, PDC_COR, and PDC_NOI) that are available in the light curve data product FITS headers; in particular, in the second FITS header of light curve data products (see [SDPDD](#)).

The CROWDSAP keyword represents the fraction of flux in the photometric aperture attributable to the target star (after background correction). A low value for CROWDSAP indicates that other stars contribute a significant amount of flux to the target and the light curve may not isolate variability for the target star of interest.

The keywords PDC_TOT, PDC_COR, and PDC_NOI assess the quality of the PDC cotrending procedure. Values of the PDC keywords range from 0.0 to 1.0, with values towards 1.0 indicating a high quality of the PDC cotrending outcome (KDPH; §8.3.3.XIV). The correlation goodness metric (PDC_COR), is calibrated such that a value greater than 0.8 means there is less than 10% mean absolute correlation between the target under study and all other targets on the CCD. The introduced noise metric (PDC_NOI) is calibrated such that a value greater than 0.8 means the power in broad-band introduced noise is below the level of uncertainties in the flux values. The total goodness metric (PDC_TOT) provides an overall summary of the cotrending quality.

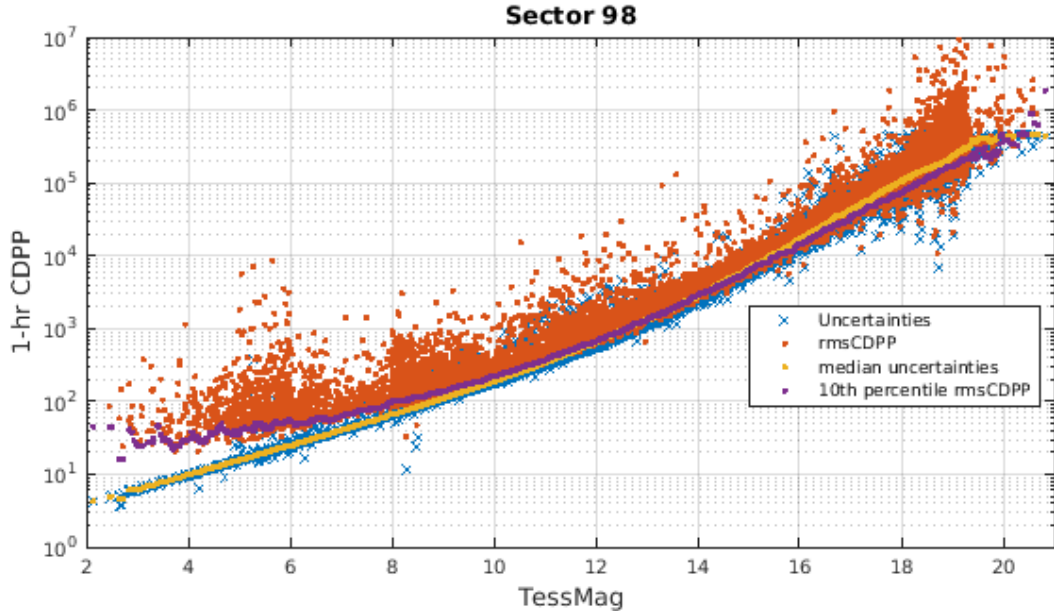


Figure 5: 1-hour CDPP. The red points are the RMS CDPP measurements for the 12992 light curves from Sector 98 plotted as a function of TESS magnitude. The blue x’s are the uncertainties, scaled to 1-hour timescale. The purple curve is a moving 10th percentile of the RMS CDPP measurements, and the gold curve is a moving median of the 1-hr uncertainties.

2.2 Transit Search and Data Validation

In Sector 98, the two-minute light curves of 12992 targets were subjected to the transit search in TPS. Of these, Threshold Crossing Events (TCEs) at the 7.1σ level were generated for 1019 targets.

We employed an iterative method when conducting the Sector 98 transit search. The top panel of Figure 6 shows the number of TCEs at a given cadence that exhibit a transit signal from an initial run of TPS. The $3\text{-}\sigma$ peaks were used to define de-emphasis weights for a second run of TPS, the results of which are shown in the bottom panel of Figure 6. The final set of TCEs and the results reported here are based on the second run of TPS. The values of the adopted de-emphasis weights are provided in the DV timeseries data products for targets with TCEs.

The top panel of Figure 7 shows the distribution of orbital periods for the final set of TCEs found in Sector 98. The rise in the period distribution beyond ~ 10 days is due, in part, to a large number of two-transit detections, many of which are likely false positives. Two-transit TCEs can be identified with the `NTRANS` keyword in the headers of the dv-timeseries FITS files. The vertical histogram in the right panel of Figure 7 shows the distribution of transit depths derived from limb-darkened transiting planet model fits for TCEs. The model transit depths range down to the order of 100 ppm, but the bulk of the transit depths are considerably larger.

A search for additional TCEs in potential multiple planet systems was conducted in DV through calls to TPS. A total of 1441 TCEs were ultimately identified in the SPOC pipeline on 1019 unique target stars. Table 3 provides a breakdown of the number of TCEs by target.

Note that targets with large numbers of TCEs are likely to include false positives.

Table 3: Sector 98 TCE Numbers

Number of TCEs	Number of Targets	Total TCEs
1	707	707
2	241	482
3	48	144
4	13	52
5	4	20
6	6	36
–	1019	1441

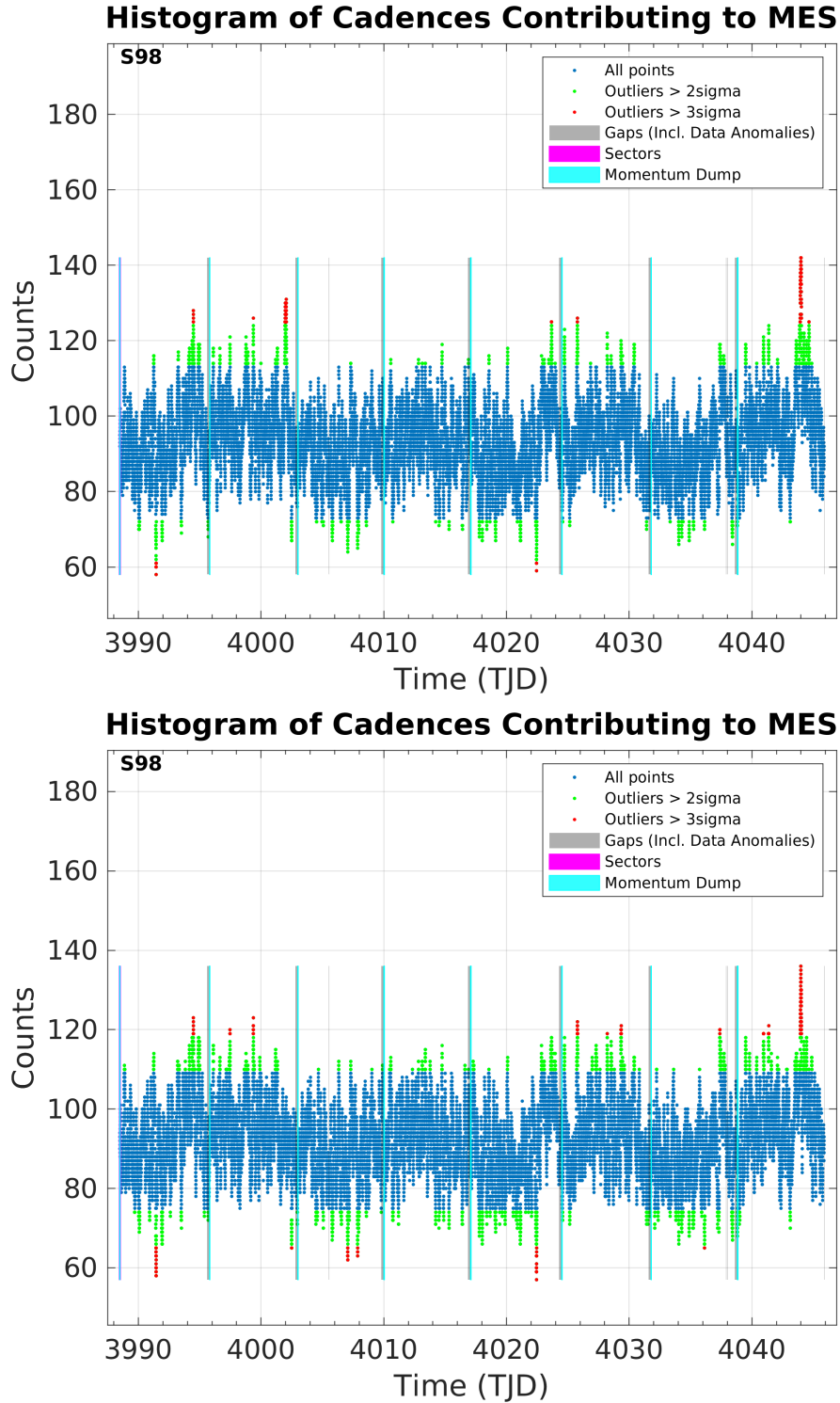


Figure 6: Top panel: Number of TCEs at a given cadence exhibiting a transit signal, based on an initial run of TPS. Any isolated peaks are caused by single events that result in spurious TCEs. These peaks were used to define de-emphasis weights that suppress problematic epochs for the transit detection statistics in a second iteration of TPS. Bottom panel: Results from the second run of TPS.

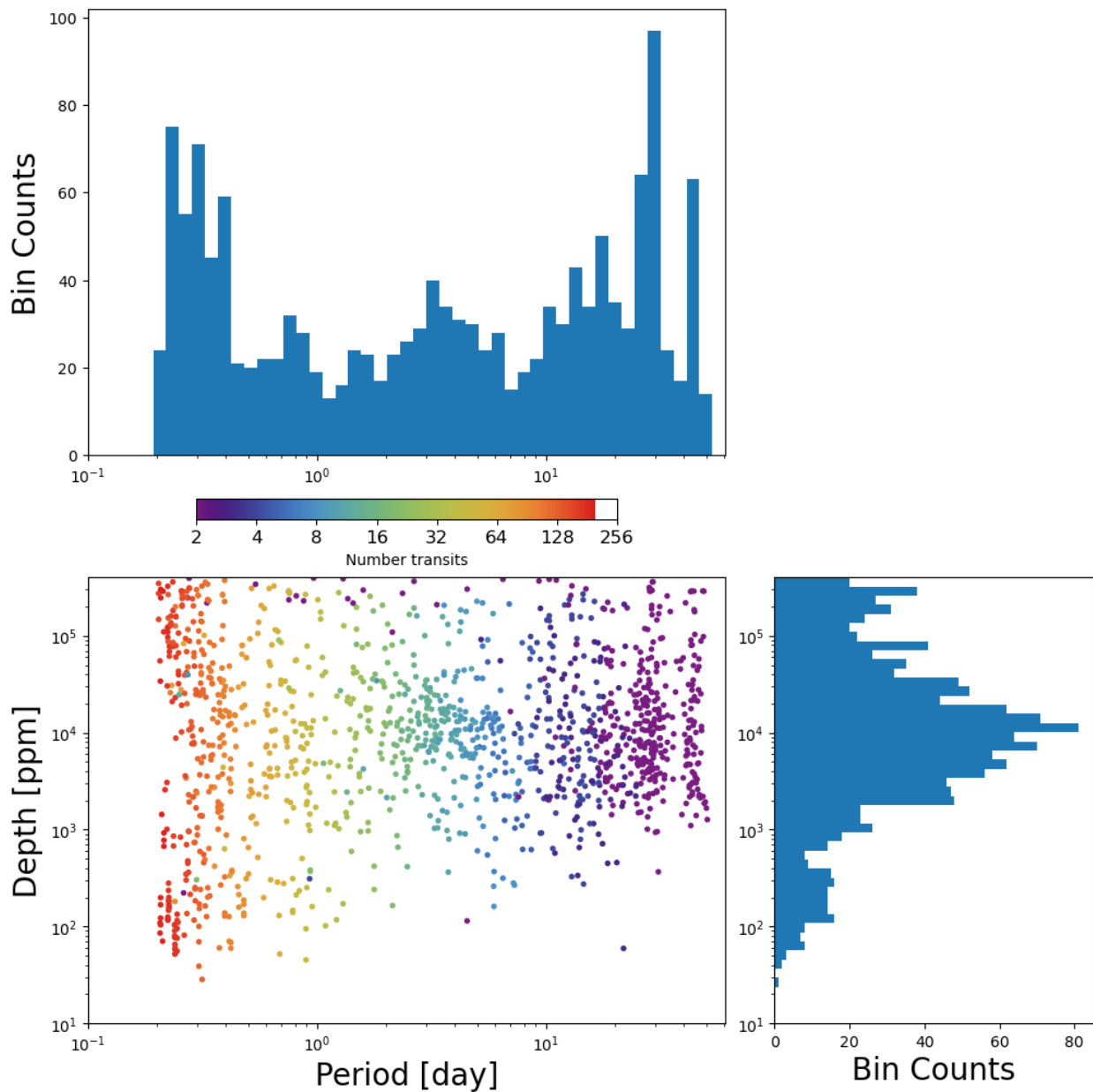


Figure 7: Lower Left Panel: Transit depth as a function of orbital period for the 1441 TCEs identified for the Sector 98 search. Reported depth comes from the DV limb-darkened transit fit depth when available, and the DV trapezoid model fit depth when not available. The number of observed transit events for each TCE is indicated by point color. Top Panel: Orbital period distribution of the TCEs shown in the lower left panel. Right Panel: Transit depth distribution for the TCEs shown in the lower left panel.

Appendix A: Details of Data Anomaly Flags

See the [SDPDD](#) (§9) for a list of data quality flags and the associated binary values used for TESS data.

The following flags are set by hand, based on mission operations and spacecraft telemetry: bits 1 and 2 (Attitude Tweak and Safe Mode).

Cadences marked with bits 3, 4, 6, and 12 (Coarse Point, Earth Point, Reaction Wheel Desaturation Event, and Predicted Straylight) are flagged based on spacecraft telemetry. Cadences marked with bits 2 and 4 (Safe Mode and Earth Point) have NULL values for the timestamps and data in the target-pixel files and light curve files.

Note that just after the data downlinks near apogee (midpoint of each orbit), the spacecraft pointing is still settling for 20 to 60 seconds after data collection resumes. Cadences during this time are marked with bit 8 (Manual Exclude, described below).

Cadences marked with bit 5 and 10 (Argabrightening Events and Impulsive Outlier) were identified by the SPOC pipeline. Bit 5 marks a sudden change in the background measurements. In practice, bit 5 flags are caused by rapidly changing glints and unstable pointing at times near momentum dumps. Bit 10 marks an outlier identified by PDC and omitted from the cotrending procedure.

The 20-second data mode includes cadences marked with bit 7 and 11 (Cosmic Ray in Optimal Aperture and Cosmic Ray in Collateral Pixel). These flags indicate cadences affected by cosmic rays that are removed by the pipeline, and can be found in both the TPF and LC files. The data provided in the archive products are corrected for cosmic rays, and a FITS table extension in the TPF and Collateral Pixel File details the cosmic rays identified and removed by the pipeline at the pixel level.

Cadences marked with bit 8 (Manual Exclude) are ignored by PDC, TPS, and DV for cotrending and transit searches. These cadences were identified using spacecraft telemetry from the fine pointing system. All cadences with pointing excursions >7 arcsec (0.3 pixel) were flagged for manual exclude. These cadences can also be set manually in order to identify off-nominal data collection (e.g., engineering tests, spacecraft anomalies, etc).

The predicted stray light flag (bit 12, value 2048) is marked in the FFIs and flags times when the Earth/Moon are near the camera FOVs and may interfere with guiding or saturate the detectors. We strongly recommend that users inspect the FFI data before removing images marked with bit 12, as this flag is set based on predictions from mission planning and is known to be conservative with respect to the quality of data usable for analysis. This flag is disabled for the 2-minute and 20-second data products.

The scattered light exclude flag (bit 13, value 4096) identifies cadences at which individual targets are affected by scattered light.

If the Earth/Moon interference is strong enough to saturate the detector, all targets on a CCD slice will be affected and the data are unusable. Cadences with bad calibrations due to saturation are now explicitly marked with bit 15 (value 16384, “Bad Calibration Exclude”). For some cadences, the majority of targets on a CCD may be flagged for scattered light and not enough valid data remains to derive cotrending basis vectors in PDC. No systematic error correction can be applied at these times. This situation is identified by bit 16 (value 32768, “Insufficient Targets for Error Correction Exclude”).

FFIs were only marked with bits 3, 4, 6, 8, 12, and 15 (Coarse Point, Earth Point,

Reaction Wheel Desaturation Events, Manual Exclude, Straylight, and Bad Calibration Exclude). There are no WCS coordinates for FFIs that coincide with momentum dumps (bit 6).

References

- Jenkins, J. M. 2020, [Kepler Data Processing Handbook](#): Overview of the Science Operations Center, Tech. rep., NASA Ames Research Center
- Jenkins, J. M., Twicken, J. D., McCauliff, S., et al. 2016, in Proc. SPIE, Vol. 9913, Software and Cyberinfrastructure for Astronomy IV, [99133E](#), doi: [10.1117/12.2233418](#)
- Li, J., Tenenbaum, P., Twicken, J. D., et al. 2019, *PASP*, 131, 024506, doi: [10.1088/1538-3873/aaf44d](#)
- Twicken, J. D., Catanzarite, J. H., Clarke, B. D., et al. 2018, *PASP*, 130, 064502, doi: [10.1088/1538-3873/aab694](#)
- Vanderspek, R., Doty, J., Fausnaugh, M., et al. 2018, [TESS Instrument Handbook](#), Tech. rep., Kavli Institute for Astrophysics and Space Science, Massachusetts Institute of Technology

Acronyms and Abbreviation List

BTJD	Barycentric-corrected TESS Julian Date
CAL	Calibration Pipeline Module
CBV	Cotrending Basis Vector
CCD	Charge Coupled Device
CDPP	Combined Differential Photometric Precision
COA	Compute Optimal Aperture Pipeline Module
CSCI	Computer Software Configuration Item
CTE	Charge Transfer Efficiency
Dec	Declination
DR	Data Release
DV	Data Validation Pipeline Module
DVA	Differential Velocity Aberration
FFI	Full Frame Image
FIN	FFI Index Number
FITS	Flexible Image Transport System
FOV	Field of View
FPG	Focal Plane Geometry model
KDPH	Kepler Data Processing Handbook
KIH	Kepler Instrument Handbook
KOI	Kepler Object of Interest
MAD	Median Absolute Deviation
MAP	Maximum A Posteriori
MAST	Mikulski Archive for Space Telescopes
MES	Multiple Event Statistic
NAS	NASA Advanced Supercomputing Division
PA	Photometric Analysis Pipeline Module

PDC Presearch Data Conditioning Pipeline Module

PDC-MAP Presearch Data Conditioning Maximum A Posteriori algorithm

PDC-msMAP Presearch Data Conditioning Multiscale Maximum A Posteriori algorithm

PDF Portable Document Format

POC Payload Operations Center

POU Propagation of Uncertainties

PPA Photometer Performance Assessment

ppm Parts-per-million

PRF Pixel Response Function

RA Right Ascension

RMS Root Mean Square

SAP Simple Aperture Photometry

SDPDD Science Data Products Description Document

SNR Signal-to-Noise Ratio

SPOC Science Processing Operations Center

SVD Singular Value Decomposition

TCE Threshold Crossing Event

TESS Transiting Exoplanet Survey Satellite

TIC TESS Input Catalog

TIH TESS Instrument Handbook

TJD TESS Julian Date

TOI TESS Object of Interest

TPS Transiting Planet Search Pipeline Module

UTC Coordinated Universal Time

WCS World Coordinate System

XML Extensible Markup Language